LOSSLESS CONTOUR REPRESENTATION USING EFFICIENT MULTIPLE GRID CHAIN CODING

Heechan Park, Graham R. Martin, Andy C. Yu

Department of Computer Science
University of Warwick, Coventry United Kingdom
email: {heechan, grm, andycyu}@dcs.warwick.ac.uk

ABSTRACT

We present an efficient lossless contour coding scheme based on a chain code representation. The algorithm is suitable for the binary shape coding of arbitrarily-shaped objects. Previous attempts to exploit the correlation between successive chain links have resulted in a complex encoding process, due either to the employment of chain code post processing or by dividing the contour into segments. Our approach exploits the differential predictability of contour smoothness by embedding it into the chain structure. Anisotropic chain links are applied in the direction of the contour according to selection rules that exploit contour coherence effectively. Experimental evaluation indicates that the proposed algorithm provides superior performance over existing chain coding schemes, and implementation complexity is not increased.

1. INTRODUCTION

The lossless encoding of an arbitrarily-shaped binary contour has applications in cartography, medical image processing and computer graphics. It is also a requirement for shape representation in objectbased video coding, for example in the MPEG-4 standard[1]. We focus on the chain coding technique pioneered by Freeman[2], due to its simplicity and high performance. Chain coding is based on the fact that successive points on a digitized continuous curve are adjacent to each other, and that each data point in sequence is adjacent to one of the eight grid points surrounding the current point. A directed line segment connecting two adjacent grid points is called a link, and a chain is defined as an ordered sequence of links.

Differential chain code[3], an extension of the technique developed by Freeman, can offer substantial improvements in encoding efficiency. There have been various attempts to improve the efficiency of differential chain codes. Generalized chain codes[4] use links of different length and different angular resolution. Kaneko and Okudaira[5] proposed an algorithm in which the contour is first divided into a sequence of segments. The smoother the contour, the longer the segments employed, and hence, the higher the coding efficiency. Lu and Dunham[6] used Markov models to describe the structure of the chains, where the differential chain code is considered a Markov source.The latter two approaches attempt to exploit contour coherence, however both lead to a complex encoding process. Recently, a quasi-lossless chain coding method has been proposed, termed multiple grid chain coding (MGCC)[7]. The technique extends differential chain coding by encoding more than one pixel at a time using a hexagonal grid. We present a lossless contour encoding algorithm which shares the hexagonal grid structure of MGCC and the idea that the smoother contour, the more predictable it is, as exploited by [5]. Our approach attempts to embed the idea into a general chain structure, leading to a much simpler coding process and higher efficiency.

In the following section we summarise the MGCC method of Nune, et al[7] and identify its limitations. In section 3 we proposed a lossless MGCC algorithm that uses anisotropic cells, and a comparative evaluation is provided in section 4. Finally, some conclusions are drawn.

2. MULTIPLE GRID CHAIN CODING

MGCC[7] provides highly efficient quasi-lossless contour coding using a hexagonal grid, where the boundary of a shape is represented by edge sites located between adjacent pixels (Section 2.1). It offers superior performance over differential chain coding and the context based arithmetic encoding[8] adopted by the MPEG-4 standard.

2.1 Hexagonal Grid

Chain coding methods rely on a contour representation to code shape information. A common approach is to describe the shape by those pixels surrounding the actual contour, defining an outer pixel based contour. In a similar way, the shape can be described by the interior pixels. Although these pixel-based descriptions allow an unambiguous representation, they require some contour elements to be coded more than once and the definition of additional chain code symbols. In order to avoid such drawbacks, MGCC adopts a hexagonal grid, as shown in Fig.1. The boundary of a shape is essentially represented by the spaces (edges) between adjacent pixels.

2.2 MGCC Cell and Selection Rule

The scheme uses a square cell of dimensions 3×3 pixels, as shown in Fig.2. Any path starting from the entry, denoted 0, to one of the exits can be encoded by the corresponding exit number $\{1, 2, \cdots, 5\}$. The method causes contour simplication, which reduces the coding requirement. However it also introduces ambiguities in the decoding process, as a coded exit can represent more than on contour configuration (path within the cell) as illustrated in Fig.3. Lossless reconstruction can be achieved by transmitting only one additional bit for each cell. MGCC employs a second, horizontally-flipped, cell type to provide adaptability based on the prediction of the contour. In other words, the type of the subsequent cell is dependent on the exit of the current cell, according to the following rule.

$$Select(Cell_{type}(n), Cell_{exit}(n)) = Cell_{type}(n+1)$$

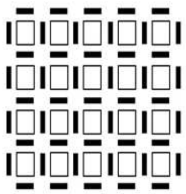

Figure 1: Hexagonal grid: dark shaded bars indicate edges

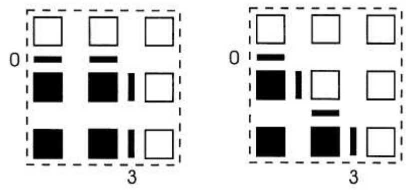

Figure 3: Ambiguities at decoding process

where n represents the cell sequence number, and the Select function is defined as

$$Select(x,y) = \left\{ \begin{array}{cc} \neg x & 1 \leq y \leq 3 \\ x & else \end{array} \right\}$$

where $\neg$ implies the other type of cell.

The cell, locally, is an optimized contour representation tool for arbitrary shapes, and providing negligible losses. The exits of each cell represent movement along the shape boundary and the hexagonal grid offers the basis for a non-redundant description of the contour. However, in a global sense, the correlation between consecutive cells is reflected in the scheme less-effectively. In MGCC, the selection rule and types of cell were initially devised so that each cell would embrace as many contour edges as possible (contour adaptability), thereby resulting in fewer bits. However, as only two types of cell are available, the selected cell is inevitably suboptimal due to a lack of directionality, while robustness is provided as the two types cover all directions. The motivation behind our proposed algorithm is to provide better directionality (more cell types) and a good selection rule supporting directionality by determining the effective cell type to be subsequently used.

3. PROPOSED APPROACH

The MGCC scheme offers two types of cell that generally leads to the robust coding of a wide range of contour variation. The idea of the new scheme is to increase coding efficiency by the directionality property and to maintain the robustness by reliable selection rules.

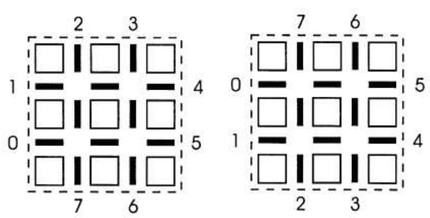

Figure 2: Cell types: (left)clockwise, (right)anti-clockwise

3.1 2×3 Cell based on Directionality and Anisotropy

In order to take advantage of the full potential of directional cell structure, an anisotropic cell type is chosen. In the sense that a cell, by the directionality, always faces the direction of the next contour, an elongation of the cell in the direction of travel, intuitively, enhances efficiency as it allows more pixels to be encoded per cell.

As mentioned, MGCC introduces ambiguities during the decoding process while one additional bit indicating path allows lossless reconstruction. The modified cell type, shown in Fig. 4, does not contain internal pixels. This removes the ambiguities that cause a distorted representation and therefore enables lossless reconstruction without overhead. The elongation creates additional cell types, depending on whether it is oriented vertically or horizontally and whether the entry point is located ahead or to the side. Fig. 4 depicts the elongated cells where the left-most two cells are categorized as $left$ cell type pointing in the same direction relative to the position of the $\{0\}$ exit, and further categorized as being elongated $vertically$ and $horizontally$. Similar classifications exist for the *right* cell types. Note that the cells shown are all of an *Ahead*-entry type. *Side*-entry cells are obtained by interchanging the positions of exits $\{0\}$ and $\{5\}$. This provides a total of eight types. The type of cell is defined by the triple:

$$Cell_{type} ::= (Cell_{hand} \times Cell_{orientation} \times Cell_{entry})$$

where *hand* refers to left and right, $orientation$ indicates whether the cell is vertical or horizontal, and $entry$ determines the position of cell entry.

3.2 Selection rule and Encoding

The cells incorporate properties of directionality and anisotropy, and corresponding reliable selection rules supporting these properties are required. We define a term fragment as being a section of contour comprising only left or only right cells using the likely exits$\{1,2,3\}$, given by

$$Fragment ::= (Direction, Seq(Cell_{LikelyExit}))$$

A complete contour is composed of a sequence of fragments. Whenever the exits $\{4,5\}$ are encountered, a new fragment begins. Dynamic cell type changes of entry and orientation can occur within a fragment. These changes are inherent to the selection rules and do not need to be coded. It is important to record the absolute direction at the beginning of each fragment but not for each individual cell as in the conventional MGCC scheme. Note that fragment is only a concept

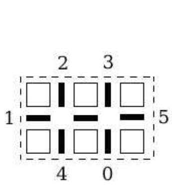

Figure 4: Lossless encoding cell types

to explain dynamic changes and does not require segmentation of the contour.

Fig.5 and Fig.6 illustrate the coding process using the overlapping rectangular cells of MGCC and the proposed scheme respectively. The selection rules for the proposed scheme are given below. The encoding process proceeds from the bottom-left to top-right. The first cell types in the bottom-left corner are anti-clockwise and right / vertical /ahead in Fig.5 and Fig.6 respectively.

$$Select((k,l,m),n) =$$

$$\left\{ \begin{array}{ll} if & \left[\begin{array}{c} \left\{ \begin{array}{c} l = vertical \\ m = ahead \end{array} \right\} \\ or \\ \left\{ \begin{array}{c} l = horizontal \\ m = side \end{array} \right\} \end{array} \right] \\ then & \left[\begin{array}{ccc} (k,l,m) & & n \in \{1\} \\ (k,l,\neg m) & & n \in \{2\} \\ (k,\neg l,\neg m) & if & n \in \{3\} \\ (\neg k,l,\neg m) & & n \in \{4\} \\ (\neg k,\neg l,\neg m) & & n \in \{5\} \end{array} \right] \\ else & \left[\begin{array}{ccc} (k,l,\neg m) & & n \in \{1\} \\ (k,\neg l,\neg m) & if & n \in \{2,3\} \\ (\neg k,l,m) & & n \in \{4\} \\ (\neg k,\neg l,\neg m) & & n \in \{5\} \end{array} \right] \end{array} \right\}$$

4. EXPERIMENTAL EVALUATION

The proposed scheme is compared with Freeman's chain code, Differential chain code, MGCC lossless and MGCC quasi-lossless. Evaluation of the chain coding schemes is performed using the binary-segmented MPEG-4 test sequences "Container", "Children", "Weather" and "Stefan", each in CIF resolution. Each sequence exhibit a different degree of contour complexity. "Children" is the most complex, followed by Container, Stefan, then Weather. The contour element where the shape encoding starts is the first active edge site found when scanning the contour image from left to right and top to bottom. Therefore, the first active site is always a horizontal element and thus the initial direction for the encoding process can be set to EAST. Note that the decoder shares this information and, therefore, it does not have to be transmitted. The position of the first initial element is coded in an absolute way, however the bit rate results in Table.1 for pure chain exclude the initial element position. At each step of searching for the next active edge site, edges are tested in the following direction order: right, ahead and left. When the encoder reaches the initial element of the current contour, the process is terminated and the exit numbers are Huffman encoded. Note that the exit edge of the last cell may not correspond with the initial edge. In decoding, from initial element the contour is tracked by decoding next available chain code until the initial element is reached.

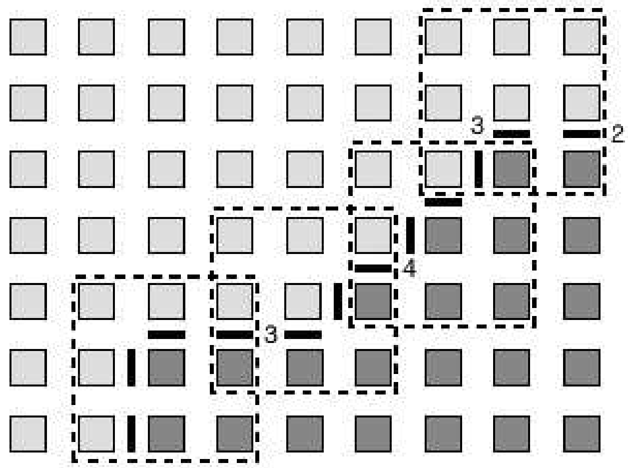

Figure 5: Example of MGCC encoding process(number denotes exit taken for each cell)

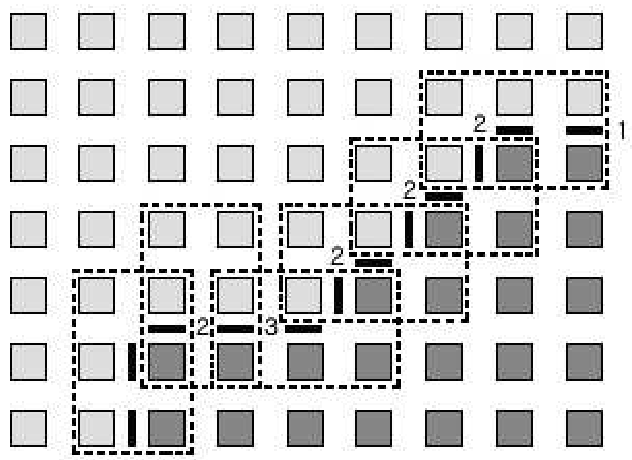

Figure 6: Example of proposed scheme

As shown in Table.1, the performance of our proposed scheme varies depending on the test sequence. For the complex contour sequence, "Children", gains of 37% over Freeman's chain code and 6% over Differential chain code are achieved. The video object in the "Weather" sequence has a comparatively smooth contour, and as expected the proposed scheme provides superior performance, gains of 58% and 24% respectively. Note that it even outperforms lossy MGCC by 5% and without loss of information. For "Stefan", the proposed scheme shows bit rate improvements of 43% and 9% over Freeman and Differential coding respectively.

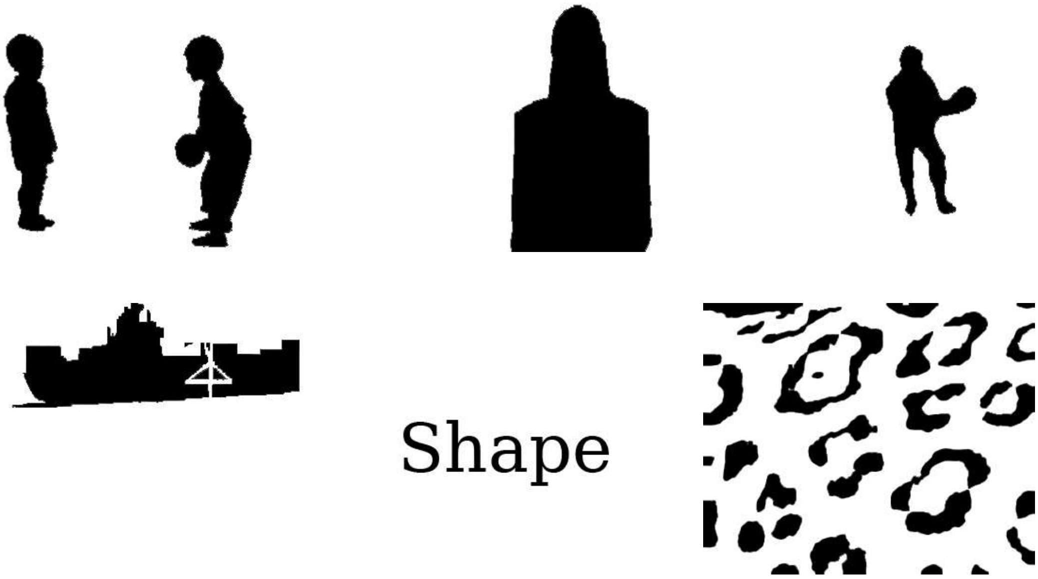

Figure 7: Experimental image sequences :(from left to right, top row first) children, weather, stefan, container, shape(still image), jaguar(still image)

Scheme	Children	Weather	Stefan
Freeman	3220.5	2141.8	1287.5
Differential	2143.2	1176.9	799.5
MGCC Lossless	2327.5	1359.6	862.8
MGCC Lossy	1682.6	944.8	613.1
Proposed Lossless	2020.6	892.6	728.7
	Container	Shape	Jaguar
Freeman	2984.6	3318	12720
Differential	1881.2	2096	8141
MGCC Lossless	2164.3	2280	8605
MGCC Lossy	1505.9	1593	6106
Proposed Lossless	1361.7	1637	7006

Table 1: Experimental Results: average bitrate per frame, over 300 frames

Surprisingly, our lossless scheme shows better compression rates than lossy MGCC, even with "Container" which exhibits abrupt changes in curvature. Further evaluations on the single image," Shape" and "Jaguar", demonstrate consistent performance over other algorithms.

5. CONCLUSION

We have described a novel lossless chain coding scheme that exploits contour coherence in an effective manner. The algorithm uses a collection of anisoptropic cells that incorporate a directionality property, and the types of cell used to represent any section of the contour are chosen according to simple self-selection rules. This minimizes the coding overhead. The sequence of cell exit identifiers is recorded and the information is Huffman coded. Contour coherence is exploited at the chain structure level, rather than relying on entropy coding to reduce redundancy in the representation. The algorithm performs significantly better than known chain coding techniques. Bit rate savings of up to 28% are demonstrated over Differential chain code, and with a similar level of computational complexity. Savings over Freeman's chain code varied from 37% to 58% for the test sequences used. The work can be further extended by using an adaptable cell size structure and more flexible selection rules. The use of arithmetic code to represent the sequence of cell exit identifiers may improve efficiency further.

REFERENCES

[1] ISO/IEC 14496-2:2004, *Information technology - coding of audio visual objects - Part 2 : Visual*, June 2004.

[2] H. Freeman, "On the encoding of arbitrary geometric configuration," *IRE Trans. Electron. Comput.*, vol. 10, pp. 260–268, 1961.

[3] H. Freeman, "Computer processing of line drawing images," *Computing Surveys*, vol. 6, 1974.

[4] J. Saghri and H. Freeman, "Analysis of theprecision of generalized chain codes for the representation of planar curves," *IEEE Trans. PAMI.*, vol. 3, pp. 533–539, 1981.

[5] T. Kaneko and M. Okudaira, "Encoding of arbitrary curves based on chain code representation," *IEEE Trans. Commun.*, vol. 33, no. 7, pp. 697–707, July 1985.

[6] C. Lu and J. Dunham, "Highly efficient coding schemes for conour lines based on chain code representation," *IEEE Trans. Commun.*, vol. 39, no. 10, pp. 1511–1514, October 1991.

[7] P. Nune, F. Marques, F. Pereira, and A. Gasull, "A contour-based approach to binary shape coding using a multiple grid chain code," *Image Commun.*, vol. 15, pp. 585–599, 2000.

[8] N. Brady, "MPEG-4 standardized methods for the compression of arbitrarily shape video objects," *IEEE Trans. CSVT.*, vol. 9, no. 8, pp. 1170–1189, December 1999.